Available online at www.sciencedirect.com
ScienceDirect
Journal of Magnetic Resonance 187 (2007) 314–319
JMR Journal of Magnetic Resonance
www.elsevier.com/locate/jmr

Spin-glass-like magnetic ordering in Zn substituted magnetite magnetic fluids

R.V. Upadhyay [a], Kinnari Parekh [b], R.V. Mehta [a,*]

[a] Department of Physics, Bhavnagar University, Bhavnagar 364 002, India
[b] Department of Physics, Faculty of Science, M.S. University of Baroda, Vadodara, India

Received 18 January 2007; revised 14 April 2007
Available online 24 May 2007

Abstract

Electron spin resonance (ESR) spectra of magnetic fluids involving polydispersed $Zn_{0.5}Fe_{0.5}Fe_2O_4$ (FZ5) and $Zn_{0.7}Fe_{0.3}Fe_2O_4$ (FZ7) nanomagnetic particles are scanned from 4.2 to 300 K. The FZ7 fluid exhibits certain distinct features below 40 K which are different from FZ5 fluid. These include (i) an isotropic shift in resonance field in zero-field-cooled ESR study, (ii) deviation of resonance field from $\sin^2\theta$ behavior (where θ is the angle between axis of the particle and field) in field cooled (FC) sample and (iii) abrupt increase in anisotropy field for FC sample. The results are analyzed in light of the core-shell model for nanomagnetic particles.

PACS: 76.50.+g; 75.50.mm; 75.50.Lk

Keywords: Magnetic fluids; Electron spin resonance; Spin glass

1. Introduction

The study of magnetic nanoparticles is a fertile area of research due to their diverse technological applications like, high density information storage, biomedical materials, catalysis and as an active component in magnetic fluids (a colloidal suspension of nanomagnetic particles in a nonmagnetic carrier liquid), etc [1–4]. In addition to the above applications they are also used as research tools in the areas of material physics, geology, biology and medicine. In nanomagnetic materials magnetic properties depend on the intrinsic properties of the particles and the interaction between them. The properties due to interactions are reviewed in Refs. [5,6] while Kodama [7] has reviewed intrinsic properties of magnetic nanoparticles with special reference to the effect of finite size on zero temperature spin ordering, magnetic excitations and relaxation. Based on these reviews it is now clear that the magnetic ground state of nanomagnetic particle is strongly influenced by finite size and micro-structural details of both core and surface. Kodama et al. [8] have shown that surface spins, which endure a deficiency in exchange interaction, may play a specific role on the structure and dynamical behavior of nanomagnetic particles. A good deal of research work is devoted to understand the role of surface spin ordering in magnetic properties of nanomagnetic particles at low temperature [9–14].

Earlier, we have studied the electron spin resonance (ESR) spectra of nanomagnetic $Zn_{0.5}Mn_{0.5}Fe_2O_4$, particles dispersed in kerosene at temperature between 4.2 and 400 K [15,16]. The spectra exhibited two distinct features (i) above the melting point (T_m) of the carrier liquid, two different resonance modes co-exist viz, (a) a broad line due to ferrimagnetic resonance and (b) a sharp line at $g = 2$, due to intrinsic super-paramagnetic phase. (ii) below the melting point of the carrier liquid; zero-field-cooled (ZFC) ESR spectra exhibited an isotropic shift in resonance field below 40 K, while the field cooled (FC) spectra

* Corresponding author.
E-mail address: rvm@bahvuni.edu (R.V. Mehta).

1090-7807/$ - see front matter © 2007 Elsevier Inc. All rights reserved.
doi:10.1016/j.jmr.2007.05.010

Table 1
Magnetic properties of the magnetic fluids

Sample	Domain magnetization (emu/cc)	Log-normal median diameter (Å)	Standard deviation in log-diameter(σ)	Curie temperature (K)
$Zn_{0.5}Fe_{0.5}Fe_2O_4$ (FZ5)	200	60	0.37	364
$Zn_{0.7}Fe_{0.3}Fe_2O_4$ (FZ7)	115	43	0.25	347

showed hysteresis behavior in variation of resonance field versus θ, where θ is the angle between axis of the particle and applied magnetic field. Further, FC sample did not obey $\sin^2\theta$ behavior [16]. In both the cases (i.e., ZFC and FC) the linewidth increases sharply below 50 K. These results were analyzed using random field exchange anisotropy model as proposed by Martinez et al. [17]. Using this model it is shown that below 50 K, the surface spin-glass-like layer freezes and give rise to isotropic shift in resonance field and an unidirectional freezing property of spins shows angular dependent hysteresis for field cooled configuration [16]. Similar effects were also observed by Koksharov et al. [18,19] and Gazeau et al. [20].

The applicability of this model to other similar polydispersed nanomagnetic system is studied here. ESR spectra of polydispersed $Zn_{0.5}Fe_{0.5}Fe_2O_4$ (FZ5) and $Zn_{0.7}Fe_{0.3}Fe_2O_4$ (FZ7) nanomagnetic particles in kerosene were recorded in the temperature range 4.2–300 K. These samples also have low Curie temperature below 400 K and high pyromagnetic co-efficient [21,22]. The detailed magnetic properties of these fluids are discussed elsewhere [21,22]. Table 1 gives the certain properties of these fluids. The spectra are analyzed in light of the above model.

2. Sample characterization

$Zn_xFe_{1-x}Fe_2O_4$ particles with different concentration of Zn were synthesized using chemical coprecipitation technique. The Fe^{3+}, Fe^{2+} and Zn^{2+} ions in an aqueous solution were mixed in appropriate molar ratio in distilled water and using 8 M NaOH solution precipitate were obtained under vigorous stirring at room temperature. After the precipitation, the suspension was kept for digestion at 80 °C for 20 min. During this time, the particles grew and transformed to the crystalline state. The crystalline nature was confirmed by the X-ray diffraction technique. Oleic acid was then added and the mixture was stirred for an hour. The fluid was heated and peptized by adding a small amount of dilute HCl. By magnetic sedimentation the oleic acid coated particles was repeatedly washed with double distilled water and subsequently washed with acetone to remove water. Ultimately, this acetone wet slurry was dispersed in diester (Bis (2-ethylhexyl Adipate)). The structure of particles is determined using a BrukerD8-Advance X-ray powder diffractometer. Fig. 1 shows the XRD pattern for FZ5 and FZ7 samples. The analysis confirms the formation of single phase cubic spinel structure. The particle size (diameter) determined by Scherrer's formula for (311) reflection are 53 and 40 Å, for FZ5 and FZ7 samples, respectively.

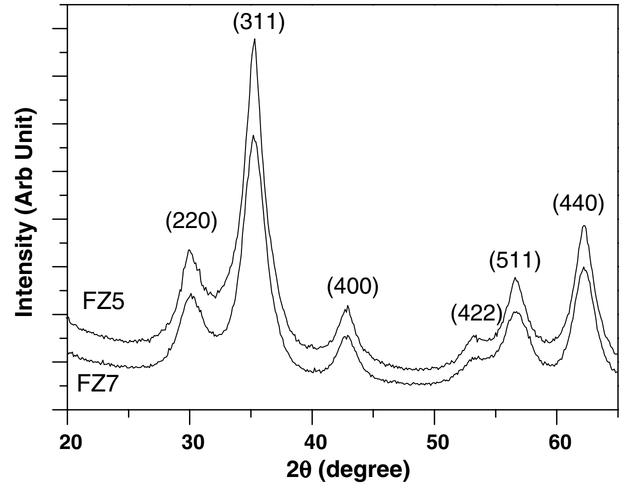

Fig. 1. XRD pattern for FZ5 and FZ7 sample.

The room temperature magnetization curves for FZ5 and FZ7 magnetic fluids (Fig. 2) exhibit zero remanence and coercivity. Using the log normal size distribution of particle volume and Langevin's theory the magnetization results are analyzed and values thus obtained for FZ5 and FZ7 fluids are given in Table 1.

3. Esr measurements

ESR measurements are carried out using Bruker-ESR spectrometer operating at an X-band frequency (9–10 GHz). A 10 Gauss modulation field is used at 100 kHz frequency, this does not cause any distortion at low temperature in the line shape. The original fluid (volume frac-

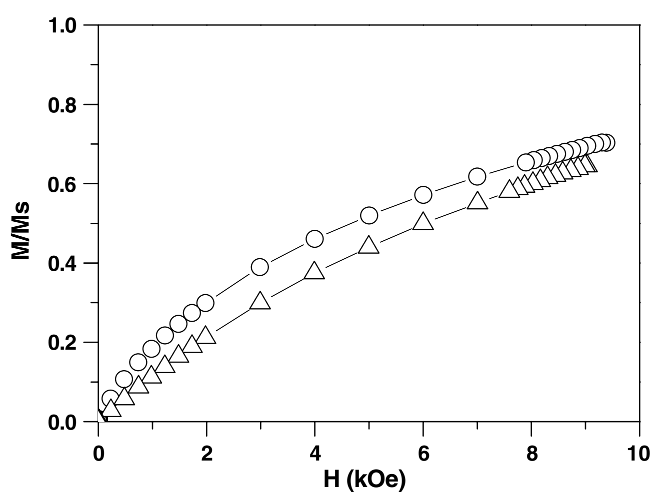

Fig. 2. Magnetic response of magnetic fluids at room temperature for FZ5 (○) and FZ7 (△) samples.

tion of the fluids are 5% and 7%, for FZ5 and FZ7 magnetic fluids, respectively) is diluted 100 times in order to decrease the interparticle interaction as well as to prevent the radio frequency field line distortion.

In ZFC measurements, the system is initially cooled in absence of magnetic field from 300 to 4.2 K and then the ESR patterns were recorded by scanning the field in warming up cycle. In case of FC measurements a 10 k Oe dc-magnetic field is applied to the sample at 300 K and then cooled to 4.2 K under the influence of magnetic field. The later leads to the freezing of angular orientation of the magnetic moment of particle in the direction of the magnetic field. Thus the medium will be textured. This will freeze the orientation of all the particles and the medium will be textured. The angle dependent ESR measurements were recorded by rotating the Dewar insert containing the FC sample at various angles (θ) with respect to the applied magnetic field direction.

At low temperature, the observed linewidth (ΔH_{pp}) is large (>1500 Oe) therefore one has to take into account the relaxation phenomenon in the analysis. Considering the Landau–Lifshitz formulation and assuming that the observed pattern is due to the super-positions of microwave absorption of identical ellipsoidal particles (i.e., with the same form factor, magnetization and relaxation factors) one obtains [23]

$$H_{res} = H^1_{res} + \frac{3}{4}\left(\frac{\Delta H^2_{pp}}{H_{ref}}\right) \quad (1)$$

Here, H_{res} H^1_{res} and H_{ref} are respectively, the resonance fields without relaxation effect, with relaxation effect and reference resonance field. In the present case the reference resonance field is 3400 Oe. The resonance field values used in the analysis are corrected using Eq. (1).

4. Results and discussion

4.1. Randomly oriented easy axis: ZFC condition

Typical ESR spectra for $x = 0.5$ and 0.7 fluid samples recorded at different temperatures are shown in Fig. 3a and b. All the spectra were analyzed using Lorentzian distribution function and the parameters like resonance field, H_r, peak-to-peak linewidth, ΔH_{pp}, area under the curve, etc., were obtained. The deconvolution of the spectra show that each spectrum is a super-position of two resonance modes: a broad line and a sharp line at $g = 2$. Such two resonance modes feature was also observed by earlier workers [16,24–27]. The variation of peak-to-peak linewidth (ΔH_{pp}) and resonance field (H_{res}) with temperature for ZFC (randomly oriented easy axis) are plotted in Fig. 4. In the case of FZ5, the linewidth increases gradually with decrease in temperature, while for FZ7 it shows a sudden increase below 50 K. Similarly, resonance field remains almost invariant from 4.2 to 200 K for FZ5 fluid while for FZ7 fluid, resonance field remains constant for $T > 40$ K and

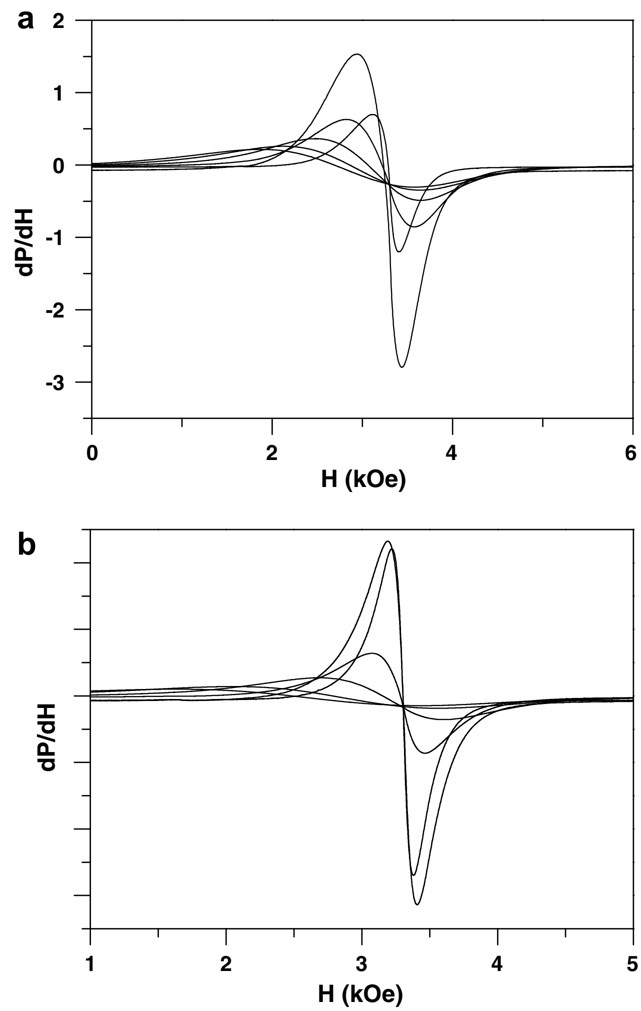

Fig. 3. First derivative of power absorption as a function of field at different temperatures viz; 20, 40, 100, 180, 260 and 300 K. For (a) FZ5 and (b) FZ7 sample.

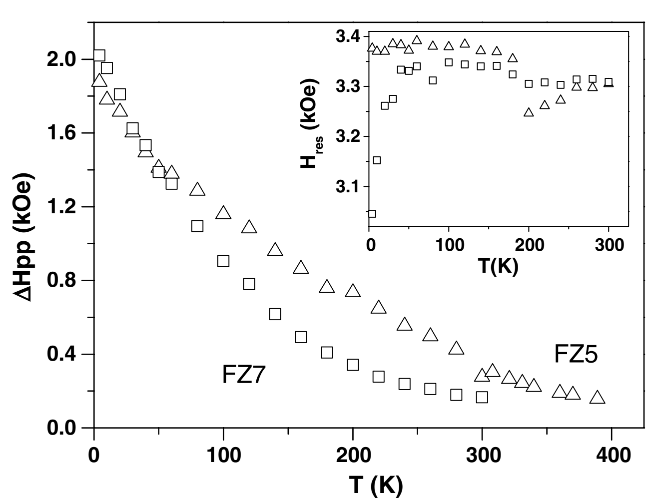

Fig. 4. Variation of the peak-to-peak linewidth (ΔH_{pp}) with temperature for a randomly oriented easy axis samples of FZ5 (△) and FZ7 (□) magnetic fluids. Inset: variation of resonance field (H_r) after correcting for the relaxation effect using Eq. (1) with temperature for FZ5 (△) and FZ7 (□) magnetic fluids.

thereafter it decreases. Similar behavior was also observed in Mn–Zn sample [16]. The observed discontinuity at $T = 200$ K, is due to the melting of the carrier, and above this temperature the randomly frozen anisotropy axis will now free to orient in the medium. The system approaches towards the super-paramagnetic state with increasing temperature. The increase in the linewidth with decreasing temperature is attributed to the distribution of internal local fields because temperature dependence of energy barriers due to dipole–dipole field energy, anisotropy energy and dipole field energy are different.

At the temperature below 40 K, FZ7 system shows increases in linewidth with decrease in temperature (Fig. 4) while the resonance field decreases with decrease in temperature. This behavior is similar to that described by other workers [18–20]. It may be noted that these features cannot be accounted by the dipole–dipole interaction as the inter-particle distance for the diluted sample used in the study leads to the magnitude of the dipole–dipole energy to less than 1 K. On the other hand it has been observed that for a system with spin-glass-like transition the ESR linewidth usually exhibits broadening below the spin glass temperature. Using this argument, earlier workers have explained origin of this isotropic shift in resonance field—i.e., $[H_{iso} = H_{ref} - H_{res}(\mathrm{ZFC})]$ and additional line broadening as due to the intrinsic spin-glass-like state which takes place on the surface of an individual particle at low temperature.

In our earlier study on Mn–Zn system [16] it was shown that the observed isotropic shift and increase in linewidth for $T < 40$ K can be accounted by considering the particle to have a ferromagnetic core and surface spin-glass-like layer. The former changes its orientation by coherent rotation while the later slowly relaxes in the direction of the field. In the present case the observed isotropic shift value (~350 Oe) is much smaller than that observed for Mn–Zn system (1500 Oe) at 4.2 K. Apart from the different magnetic properties of the systems one of the reason may be the particle size, which for Mn–Zn system was 68 Å while for the FZ7 sample it is 43 Å. Thus one can argue that in the present case the properties are more dominated by surface spins than core. This feature is more pronounced in the field cooled ESR study.

4.2. Preferred oriented easy axis: FC condition

When a magnetic fluid is cooled from 300 to 4.2 K under the influence of 10 k Oe dc-magnetic field the anisotropy axis of the majority of the particles will be aligned along the field cooled direction and the maximum texture will be achieved. For a completely aligned system, H_{res} for parallel and perpendicular configuration is given by [20]

$$H_{res}(\|) = H_{ref} - H_a \tag{2}$$

and

$$H_{res}(\perp) = H_{ref} + \tfrac{1}{2}H_a \tag{3}$$

Thus for the randomly oriented system the average—i.e. $\langle[\{2H_{res}(\perp) + H_{res}(\|)\}/3]\rangle$—is equal to H_{ref}. The variation of resonance field with temperature for FZ5 and FZ7 are shown in Fig. 5a and b, respectively. The observed variation of resonance field with temperature for FZ5 system can be accounted by considering Eqs. (2) and (3). In case of FZ7, H_{res}, decreases with temperature for both the configurations. This suggests a different type of magnetic ordering in FZ7 below 40 K.

The variation of anisotropy field (H_a) with temperature for FZ7 (calculated using Eqs. (2) and (3)) shows an abrupt increase in H_a below 40 K (Fig. 6), while for FZ5 sample it shows a gradual increase below 40 K (Inset Fig. 6). This

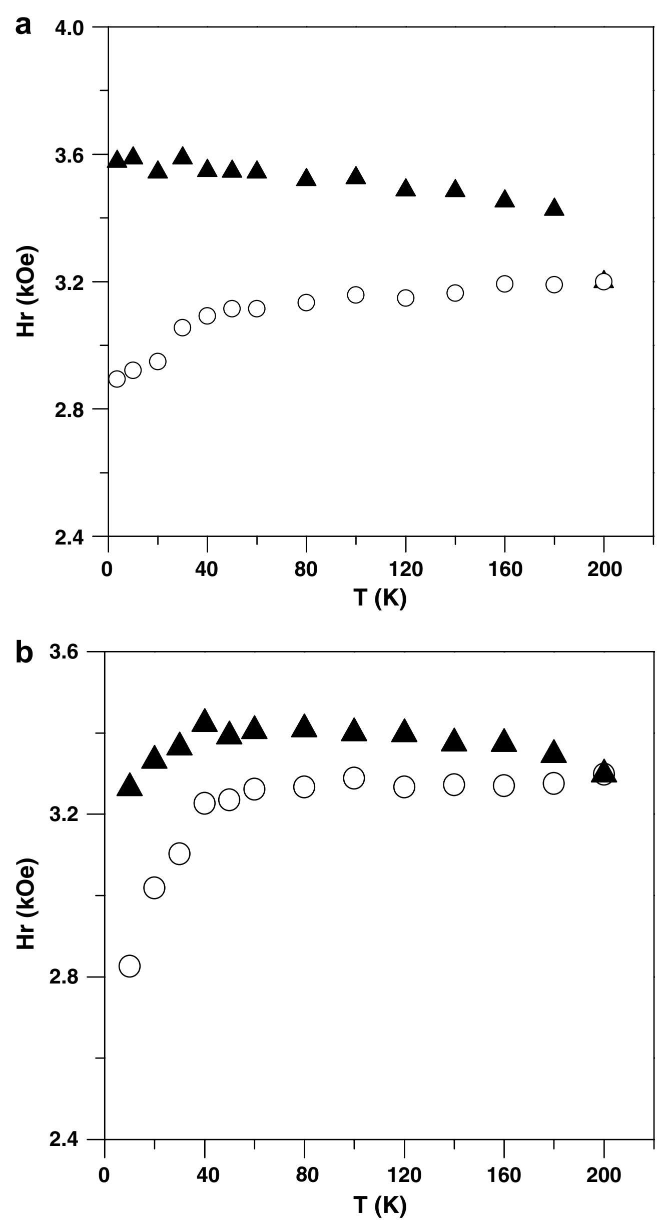

Fig. 5. (a) Resonance field variation with temperature for perpendicular (solid symbol) and parallel configuration (open symbol) for the textured FZ5 fluid. (b) Resonance field variation with temperature for perpendicular (solid symbol) and parallel configuration (open symbol) for the textured FZ7 fluid.

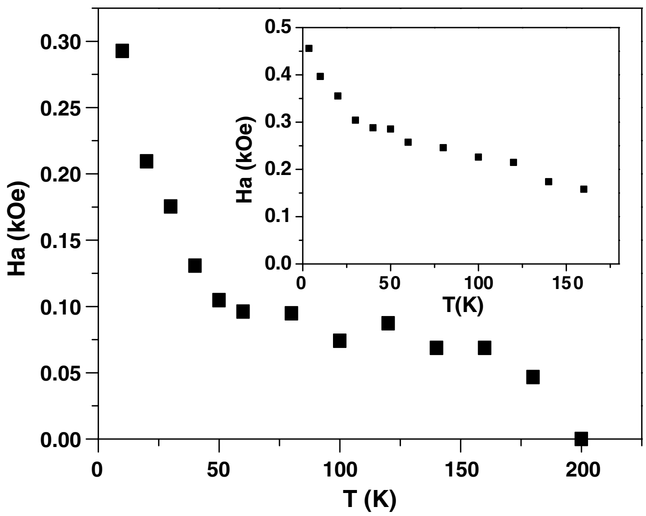

Fig. 6. Thermal variation of anisotropy field (H_a) calculated for the textured fluid of FZ7. Note the rapid increase in H_a below 50 K. (Inset: for FZ5 sample.)

again supports the concept of larger contribution of surface anisotropy in the FZ7 system compared to that in FZ5.

Generally for ferri/ferromagnetic particles, the angular dependence of the resonance field is described by the relation [28]

$$\frac{H_{\mathrm{res}}(\theta) - H_{\mathrm{res}}(0^\circ)}{H_{\mathrm{res}}(90^\circ) - H_{\mathrm{res}}(0^\circ)} = \sin^2\theta \quad (4)$$

In case of FZ5 fluid the above relation is obeyed. Hence, the system behaves as a true uniaxial system. In Mn–Zn system angular dependence hysteresis effects in resonance field was observed. To check such possibility, angular dependence resonance field for FZ5 and FZ7 textured fluids were carried out at 4.2 K. In the case of FZ7 fluid, the angular dependence showed a significant deviation from the above relation (Fig. 7). In both the cases no angular dependent hysteresis was observed.. The presence of hysteresis in Mn–Zn system [16] is due to unidirectional freezing of surface spins during field cooled condition. On removal of the field, the core experiences the field generated by the frozen surface layer in the same direction as that of the previously applied field, thus exhibits hysteresis. The absence of hysteresis in FZ7 indicates that the core relaxes back to its original position on removal of the field but the frozen surface layer give rise to large surface anisotropy (Fig. 6) below 40 K, as a result deviation from the $\sin^2\theta$ law is observed, i.e., system does not exhibit uniaxial behavior. This supports the conjecture that the because of smaller particle size, the surface dominates in FZ7 and these surface spins freezes below 40 K. Thus all the observed features in ESR spectra of FZ5 as well as FZ7 can be explained by the core-shell model used in the earlier study.

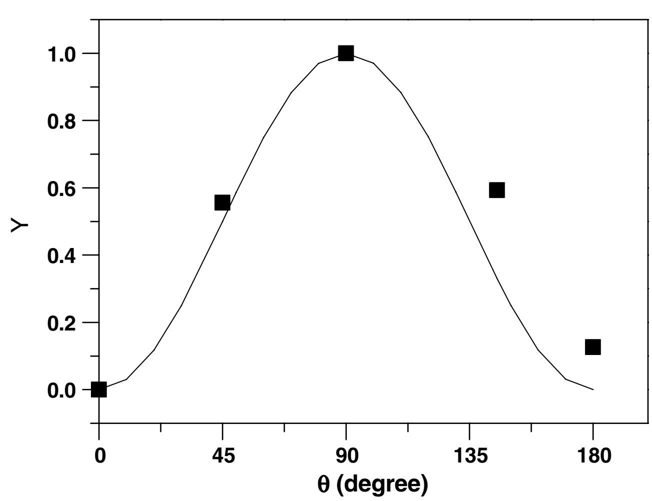

Fig. 7. Angular dependent variation of resonance field, at 4.2 K for a FZ7 field-cooled sample. The sample is cooled from 300 K i.e., in the liquid state to 4.2 K under a 10-kOe field, where $Y = [H(\theta^\circ) - H(0^\circ)]/[H(90^\circ) - H(0^\circ)]$. The data remains same from 180° to 0° orientation (i.e., no angular dependent hysteresis).

5. Summary

Using the ESR technique, it is shown that when the surface effect is dominated over that of the core, one can interpret the observed isotropic shift in resonance field, increase in anisotropy field and deviation from $\sin^2\theta$ law below 40 K in Fe–Zn systems. These data are analyzed by viewing nanomagnetic particle as monodomain core and a surface of disordered spins. The degree of disorder is a function of particle size and it freezes at low temperature and exhibits spin-glass-like magnetic ordering.

References

[1] G.C. Hadjipanayis, G.A. Prinz (Eds.), Science & Technology of Nanostructure Materials, Plenum Press, New York, 1991.
[2] J.L. Dormann, D. Fiorani (Eds.), Magnetic Properties of Fine Particles, North Holland, Amesterdam, 1992.
[3] R.E. Rosensweig, Ferrohydrodynamics, Cambridge University Press, New York, 1985.
[4] B.M. Berkovsky (Ed.), Magnetic Fluids and Applications Handbook, Begell House Publishers, New York, 1995.
[5] J.L. Dormann, D. Fiorani, E. Tranc, in: I. Pigogine, S.A. Rice (Eds.), Advances in Chemical Physics, vol. 98, Wiley, New York, 1997, p. 283.
[6] M. Hansen, S. Morup, J. Magn. Magn. Mater. 184 (1998) 262.
[7] R.H. Kodama, J. Magn. Magn. Mater. 200 (1999) 359.
[8] R.H. Kodama, A.E. Berkowitz, E.J. McNiff, S. Foner, Phys. Rev. Lett. 77 (1996) 394.
[9] A.E. Berkowitz, J.A. Lahut, I.S. Jacobs, L.M. Levinson, D.W. Forester, Phys. Rev. Lett. 34 (1975) 594.
[10] A.E. Berkowitz, J.A. Lahut, C.E. van Buran, IEEE Trans. Magn. 16 (1980) 184.
[11] J.M.D. Coey, Phys. Rev. Lett. 27 (1971) 1140.
[12] P. Prene, E. Tronc, J.P. Jolivet, J. Livage, R. Cherkaoui, M. Nogues, J.L. Dormann, Hyperfine Interact. 93 (1994) 1409.
[13] S. Linderoth, P.V. Hendriksen, F. Bodker, S. Wells, K. Devies, S. Charles, S. Morup, J. Appl. Phys 75 (1994) 6583.
[14] F. Gazeau, E. Dubois, M. Hennion, R. Perzynski, Yu.L. Raikher, Europhys. Lett. 40 (1997) 575.
[15] Kinnari Parekh, R.V. Upadhyay, R.V. Mehta, D. Srinivas, J. Appl. Phys. 88 (2000) 2799.
[16] R.V. Upadhyay, Kinnari Parekh, R.V. Mehta, Phys. Rev. B68 (2003) 224434.

[17] B. Martinez, X. Obradors, L. Balcells, A. Rouanet, C. Monty, Phys. Rev. lett. 80 (1998) 181.
[18] Yu.A. Koksharov, S.P. Gubin, I.D. Kosobudsky, M. Beltran, Y. Khodorkovsky, A.M. Tishin, J. Appl. Phys. 88 (2000) 1587.
[19] Yu.A. Koksharov, S.P. Gubin, I.D. Kosobudsky, G.Yu. Yurkov, D.A. Pankratov, L.A. Ponomarenko, M.G. Mikheev, M. Beltron, Y. Khodorkovsky, A.M. Tishin, Phys. Rev. B 63 (2000) 012407.
[20] F. Gazeau, J.C. Bacri, F. gendron, R. Perzynski, Yu.L. Raikher, V.I. Stepanov, E. Dubois, J. Magn. Magn. Mater. 186 (1998) 175.
[21] Kinnari Parekh, R.V. Upadhyay, R.V. Mehta, J. Magn. Magn. Mater. 252 (2002) 35.
[22] R. Massart, D. Zins, F. Gendron, M. Rivoire, R.V. Mehta, R.V. Upadhyay, P.S. Goyal, V.K. Aswal, J. Magn. Magn. Mater. 201 (1999) 73.
[23] A.H. Morrish, The Physical Principles of Magnetism, Wiley, New York, 1965, 549.
[24] A.L. Tronconi, P.C. Morais, F. Pelegrini, F.A. Tourinho, J. Magn. Magn. Mater. 122 (1992) 90.
[25] K. Nagata, A. Ishihara, J. Magn. Magn. Mater. 104–105 (1992) 1571.
[26] M.D. Sastry, Y. Babu, P.S. Goyal, R.V. Mehta, R.V. Upadhyay, D. Srinivas, J. Magn. Magn. Mater. 149 (1995) 64.
[27] V.K. Sharma, F. Waldner, J. Appl. Phys. 48 (1977) 4292.
[28] (a) Yu.L. Raikher, V.I. Stepanov, Sov. Phys. JETP. 75 (1992) 764;
(b) Phys. Rev. B 50 (1994) 6250;
(c) J. Magn. Magn. Mater. 149 (1995) 34.